Probing the Hydrophobic Interactions in the Skeletal Actomyosin Subfragment 1 and Its Nucleotide Complexes by Zero-Length Cross-Linking with a Nickel−Peptide Chelate†

Raoul Bertrand, Jean Derancourt, and Ridha Kassab*

Centre de Recherches de Biochimie Macromoléculaire du CNRS, ERS 155, INSERM U 249, Université de Montpellier 1, Route de Mende, BP 5051, 34033 Montpellier Cedex, France

Received March 18, 1997; Revised Manuscript Received June 2, 1997⊗

ABSTRACT: The complex of Ni(II) and the tripeptide Gly-Gly-His catalyzes, in the presence of monoperoxyphthalic acid, a zero-length protein−protein cross-linking *via* an oxidative radical pathway involving mainly aromatic amino acids and not at all nucleophilic residues [Brown, K. C., Yang, S.-H., and Kodadek, T. (1995) *Biochemistry 34*, 4733−4739]. We have taken advantage of this unprecedented cross-linking system to directly and selectively probe the solution structure and functioning of the hydrophobic interface between F-actin and skeletal myosin subfragment 1 (S-1) at the level of its aromatic components, in the absence and in the presence of nuclotides (ATP and ADP) or nucleotide analogs (AMPPNP, PP_i, and ADP·AlF_4). Following verification of the structure of the Ni(II)−peptide chelate and of its oxidized active form by electrospray mass spectrometry, complexes of F-actin and S-1 or proteolytic S-1 derivatives and complexes of S-1 and proteolytic F-actin derivatives were readily cross-linked under various controlled conditions without apparent alteration of the acto-S-1 recognition. The covalent adducts were identified on electrophoretic gels using specific protein labeling with the oxidation-resistant fluorophor, monobromobimane, combined with immunochemical staining. Two types of actin−heavy chain conjugates were produced. One, with a mass of 180 kDa, was formed in the rigor state or with ADP bound; the other one, with a mass of 200 kDa, was generated from the ternary complexes comprising a γ-P-containing ligand. They were accumulated with an efficiency of 8 and 6%, respectively. For each reversible complex, the 180 kDa:200 kDa band ratio was essentially as predicted from the nucleotide-dependent A to R equilibrium mechanism of the acto-S-1 interaction in solution [Geeves, A. M., and Conibear, P. B. (1995) *Biosphys. J. 68*, 194s−201s]. Both covalent species resulted from the cross-linking of an actin monomer to the central 50 kDa segment, and their distinct mobilities reflect γ-P-mediated structural changes at or near the actin−50 kDa fragment interface. Peptide mapping showed the cross-linking to take place between the 506−561 S-1 segment and the 48−113 actin stretch. The localization of these regions in the atomic F-actin−S-1 model implies that nucleotide-modulated close contacts, involving aromatic residues, are operating between the C-terminal helix of the hydrophobic strong actin-binding motif of S-1 bound to the primary actin monomer and the top portion of the adjacent lower actin subunit. The specificity of the nickel−peptide cross-linking, as assessed with the acto-S-1 complex, makes it a candidate for potential general use in investigations of the hydrophobic interactions within other protein motor-based assemblies.

Hydrophobic interactions at the contact interface between F-actin and the motor domain of the globular head of myosin or S-1[1] are thought to play a major role in the chemomechanical mechanism of muscle contraction. They predominate in the posthydrolytic "strong" or rigor-like state which is derived from a nucleotide-dependent isomerization of an initial prehydrolytic "weak" binding state during the ATPase cycle (*1*−*3*). The assumption by the acto-S-1 complex of the former tight binding conformation is believed to be critical to force generation as the latter process could be fueled, at least in part, by the free energy resulting from the masking of a large hydrophobic area at the acto-S-1 interface (*4, 5*). The extent and strength of the hydrophobic actin−S-1 interactions are modulated by the phosphorylation state of the nucleotide intermediate bound to the S-1 active site. Because of the communication between the acto-S-1 interface and the γ-phosphate subsite (*6*), the binding of the γ-phosphate moiety of ATP or its analogs alters, in an unknown manner, the apolar structures and bonds linking the two proteins, thereby changing the actin−S-1 affinity and enabling their cyclic interactions to take place, a feature necessary for tension development. Moreover, the energy-transducing activity of acto-S-1 in striated muscle is regulated by the relative position of tropomyosin on the thin filament that does or does not selectively interfere with the access of S-1 to its hydrophobic class of binding sites on actin (*7*−*9*). Thus, studies assessing the architecture and dynamic conformational arrangements of the apolar components of the acto-S-1 interface promise to further improve our

† This research was supported by grants from the Centre National de la Recherche Scientifique, the Institut National de la Santé et de la Recherche Médicale, and the Association Française contre les Myopathies.

* To whom correspondence and reprints requests should be addressed.

⊗ Abstract published in *Advance ACS Abstracts*, July 15, 1997.

[1] Abbreviations: S-1, myosin subfragment 1; acto-S-1, actomyosin subfragment 1; Na Dod SO_4, sodium dodecyl sulfate; ATPase, adenosine-5′-triphosphatase; MMPP, magnesium monoperoxyphthalic acid; GGH-Ni(II), the complex of Ni(II) and the tripeptide NH_2-Gly-Gly-His-COOH; MOPS, 3-(*N*-morpholino)propanesulfonic acid; HEPES, *N*-(2-hydroxyethyl)piperazine-*N*′-2-ethanesulfonic acid.

S0006-2960(97)00615-6 CCC: $14.00 © 1997 American Chemical Society

understanding of the functioning and regulation of the acto-S-1−ATP system.

The nature and location of the strong hydrophobic binding motifs of the F-actin−S-1 complex have been suggested by the atomic model of this complex which was built by fitting the tertiary structure of the two proteins to each other in accordance with assumed but not precisely determined conformational changes occurring upon complex formation (*10*, *11*). Further studies employing site-directed mutagenesis have investigated the functional participation of some of the proposed apolar recognition residues on actin (*12*) and S-1 (*13*). On the other hand, the mutational approach cannot discriminate between side chains that are facing each other at the protein complex interface and those that maintain the conformation necessary for the interaction. More direct information on the orientation of the protein surfaces and on their rearrangements upon ligand binding can be obtained from analysis of the chemically cross-linked proteins. Earlier, several cross-linking investigations of the F-actin−S-1 complex have led to the characterization of contact sites that are involved in the ionic interactions between the two proteins (*14*−*19*). Unfortunately, the employed protein cross-linkers and those so far available are unable to induce the covalent coupling of the acto-S-1 complex through its hydrophobic interface because they react only on nucleophilic groups. However, the chelate formed by the tripeptide Gly-Gly-His and Ni(II) has been recently reported to specifically catalyze, under oxidative conditions, the covalent union of associated proteins mainly *via* the aromatic side chain moieties without a contribution of any nucleophilic residue (*20*). The former functions are thought to be chemically activated as free radicals which directly react on juxtaposed unsaturated groups with the establishment of stable and zero-length bonds. This novel protein cross-linking strategy prompted us to selectively probe the apolar acto-S-1 interface at the level of its aromatic amino acids. The present work describes the GGH-Ni(II)-promoted cross-linking of the skeletal acto-S-1 in the rigor state and complexed to nucleotides or nucleotide analogs. The results reveal the cross-linking of the 48−113 actin stretch at the top region of subdomain 1 with strand of S-1 residues 506−561, including the primary strong, hydrophobic actin-binding motif and residing in the lower 50 kDa subdomain. They also illustrate the specific influence of the γ-phosphate moiety of the nucleotides on the covalent reaction. Preliminary data of this work have been reported in abstract form (*21*).

MATERIALS AND METHODS

Chemicals. The peptide Gly-Gly-His, monobromobimane, thrombin from human plasma (2450 NIH units/mg), and affinity-purified antibody directed against the 11 C-terminal residues of actin were supplied by Sigma. Nickel(II) acetate tetrahydrate and magnesium monoperoxyphthalic acid hexahydrate were purchased from Aldrich. TPCK-treated trypsin and endoproteinase Glu-C were obtained from Worthington and ICN Biochemicals, respectively. Subtilisin was from Boehringer-Mannheim.

Protein Preparations. Rabbit skeletal myosin was prepared as described (*22*). Chymotryptic S-1 was obtained according to ref 23 and was further purified over Sephacryl S300 (*24*). Rabbit skeletal F-actin was prepared by the procedure of ref 25. G-actin was obtained by depolymerization of F-actin (2 mg/mL) in G-buffer (2 mM Tris-HCl, 0.2 mM $CaCl_2$, 0.2 mM ATP, and 0.1 mM NaN_3, at pH 8.0). This solution was sonicated three times, for 1 min each time, at 0 °C, at a frequency of 20 000 Hz in a Microson XL200S cell disruptor and then centrifuged at 180000*g* for 1 h at 4 °C. The protein was labeled with monobromobimane at Cys 374 as described (*26*), and then the fluorescent G-actin was repolymerized by adding KCl and $MgCl_2$ to final concentrations of 10 and 2 mM, respectively. S-1 labeled at SH-1 with monobromobimane was produced as described (*27*).

Restricted hydrolysis of S-1 into (25−50−20 kDa)-S-1 with trypsin or into (28−48−22 kDa)-S-1 with endoproteinase Glu-C was performed following the procedure of ref 28. The tryptic conversion of S-1 (2.8 mg/mL) into (25−40−31 kDa)-S-1 (protease: S-1 weight ratio of 1:20) was carried out in the presence of a 2-fold molar excess of F-actin in 10 mM MOPS, 0.1 mM ADP, 0.1 mM $CaCl_2$, 10 mM KCl, and 2 mM $MgCl_2$ at pH 7.5 and 25 °C for 60 min. Subtilisin-split G-actin was produced and polymerized as reported (*29*). MgADP·BeF_x−F-actin was prepared and cleaved with subtilisin according to ref 30.

Monospecific polyclonal antibodies directed against the central tryptic 50 kDa fragment of the S-1 heavy chain were isolated from rabbits immunized with the conjugate of keyhole limpet hemocyanin and a synthetic peptide spanning residues 398−414 of human cardiac β-myosin heavy chain. They were affinity purified over immobilized rabbit skeletal myosin. Polyclonal antibodies directed to N-terminal amino acids 1−12 of actin were prepared from rabbit immune sera raised against the DNase I−G-actin complex (*31*). Polyclonal rat antibodies specifically directed against actin segment 40−113 were obtained and affinity purified as reported earlier (*32*).

Protein concentrations were determined spectrophotometrically with an extinction coefficient of $A^{1\%}_{280nm}$ of 7.5 cm^{-1} for S-1 or S-1 derivatives and 11.0 cm^{-1} for actin or actin derivatives.

Cross-Linking Reactions Using Oxidized GGH-Ni(II). The experiments were conducted on preformed complexes of acto-S-1 or acto-S-1 derivatives (50−75 μM; actin:S-1 molar ratio of 1:1) which were collected by centrifugation at 400000*g* for 20 min at 4 °C and resuspended, in the absence and in the presence of ATP, ADP, PP_i, AMPPNP, or ADP·AlF_4, in 50 mM Tris-HCl, 50 mM NaCl, 2 mM $MgCl_2$ (pH 7.5), and 1 mM GGH-Ni(II). The latter chelate was added from a concentrated aqueous solution, containing 100 mM nickel acetate and 100 mM peptide, which was prepared just prior to use (*20*). Protein conjugation was initiated by the addition of the oxidizing agent, MMPP, to 1 mM. After maximally 1 min at 20 °C, the chemical reaction was terminated with a 100-fold molar excess of β-mercaptoethanol over MMPP. The cross-linking process was analyzed by Na Dod SO_4−acrylamide gel electrophoresis. In some expriments, the covalent acto-S-1 complexes were separated from non-cross-linked S-1 before gel electrophoresis by centrifugation at 400000*g* for 20 min at 4 °C, after mixing with an equal volume of dissociating solution containing 50 mM MOPS, 1 M NaCl, 10 mM $MgCl_2$, and 10 mM sodium pyrophosphate at pH 8.0. The resulting protein pellet was then resuspended in 50 mM MOPS and 2 mM $MgCl_2$ at pH 7.0.

Electrophoresis and Immunoblotting. Na Dod SO_4− polyacrylamide gradient gel electrophoresis (5 to 18%) was carried out as described previously (*14*). Fluorescent bands were located in the gel by illumination with a long wave ultraviolet light before staining with Coomassie blue. Densitometric scanning of the gels was performed with a Schimadzu model CS-930 high-resolution gel scanner equipped with a computerized integrator. The following proteins were used as molecular weight markers: myosin heavy chain (220 000), the β'-subunit (165 000) and the β-subunit (155 000) of RNA polymerase, β-galactosidase (130 000), S-1 heavy chain (95 000), and actin (42 000).

Immunoblotting was done on nitrocellulose sheets (0.45 μM) according to ref 33. Protein bands comprised of actin or the 50 kDa S-1 heavy chain fragment were stained with the respective antibodies and then visualized by a peroxidase-conjugated goat anti-rabbit IgG using α-naphthol as the substrate.

ATPase Assays. The Mg^{2+}-ATPase of the covalent acto-S-1 complexes was assayed in a medium (1 mL) containing 5 mM ATP, 2.5 mM $MgCl_2$, 10 mM KCl, and 50 mM Tris-HCl (pH 8.0) using 0.75 nmol of S-1. The Mg^{2+}-ATPase of un-cross-linked S-1 obtained in the supernatant after dissociation and centrifugation was measured under similar conditions using 1 mg of F-actin and 0.50 nmol of S-1. Liberated P_i was determined colorimetrically as previously reported (*34*).

Proteolytic Digestions of the Covalent Acto-S-1 Complexes and Sequence Analyses. Following 1 min of cross-linking of F-actin−S-1 (75 μM) and the quenching of the reaction with β-mercatoethanol, the covalent acto-S-1 complexes first separated from non-cross-linked S-1 by treatment with the dissociating solution were resuspended in 50 mM MOPS at pH 7.0 and mixed with an equal volume of a depolymerization solution containing 100 mM MOPS, 1.2 M KI, 1 mM ATP, 1 mM $CaCl_2$, and 2 mM dithioerythritol at pH 8.0 (*17*). After incubation for 30 min at 4 °C, the mixtures were clarified by centrifugation, brought to 1 mM EDTA, and exhaustively dialyzed overnight at 4 °C, against 2 mM HEPES, 0.1 mM $CaCl_2$, 0.5 mM ATP, 0.2 mM dithioerythritol, and 1 mM EDTA at pH 8.0. After recentrifugation, the protein solutions were treated with thrombin at a protease: actin weight ratio of 1:25, at 25 °C for 45 min. The digests were then directly analyzed by gel electrophoresis.

Following 1 min of cross-linking between F-actin and (25−50−20 kDa)-S-1, the reaction medium was supplemented with β-mercaptoethanol, mixed with an equal volume of the dissociating solution (50 mM MOPS, 1 M NaCl, 10 mM $MgCl_2$, and 10 mM sodium pyrophosphate at pH 8.0), and the protein solution was digested with trypsin (enzyme: S-1 weight ratio of 1:25) for 90 min at 25 °C. The digestion was stopped by the addition of soybean trypsin inhibitor, and the mixture was centriguged at 400000*g* for 20 min, at 4 °C. The protein pellet was then resuspended in 50 mM MOPS and 2 mM $MgCl_2$ at pH 7.0 and submitted to the electrophoretic analysis. The resulting 60 kDa protein band was electroblotted onto a poly(vinylidene difluoride) membrane and subjected to NH_2-terminal sequencing using a Perkin-Elmer Procise 492 sequencer operated according to the manufacturer's pulsed liquid program. The NH_2-terminal sequence of the 31 kDa peptide was similarly analyzed after electrophoretic separation of the heavy chain fragments of (25−40−31 kDa)-S-1.

Mass Spectrometry. Electrospray ionization mass spectra of the GGH-Ni(II) complex before and after oxidation were acquired on a VG Trio-2000 mass spectrometer as previously described (*35*).

RESULTS

GGH-NI(II)-Promoted Cross-Linking of the Rigor Acto-S-1 Complex. In contrast to the previous cross-linking reactions which are initiated by a single, structurally well-defined protein cross-linker, the present cross-linking process requires the combination of the three reactants, GGH, Ni-(II), and MMPP, for the generation, *in situ*, of an oxidized GGH-Ni(II) complex, the actual catalyst of the reaction. Consequently, prior to the acto-S-1 cross-linking experiments, we first assessed the composition of the metallopeptide mixture before and after its oxidation with MMPP, using electrospray ionization mass spectrometry. This soft technique allows the transfer of noncovalently associated ligands present in solution to the gas phase with minimal decomposition and provides a mean of achieving their specific characterization (*36*). In particular, it has been employed to detect divalent cation-mediated complexation of peptides occurring in the solution phase (*35, 37*). Figure 1A illustrates the mass spectrum registered for the starting commercial sample of the tripeptide dissolved in water before complexation to Ni(II). It reveals the presence of four major species; three having molecular masses of 155.0 , 212.3, and 269.0 Da were assigned to His, Gly-His and Gly-Gly-His, respectively (calculated molecular mass values of 155.20, 212.25, and 269.34 Da, respectively). The fourth deconvoluted peak with the smallest molecular mass of 108.5 Da could not be identified. Upon the addition of $Ni(OAc)_2$, the spectrum recorded showed the appearance of two new peaks (Figure 1B). The first entity with a molecular mass of 325.1 Da must correspond to the GGH-Ni(II) complex whose calculated molecular mass is 326.03 Da, taking into account the deprotonation of two amide nitrogenes known to occur upon binding of a divalent cation to the tripeptide (*20*). The second species which has a molecular mass of 352.3 Da was tentatively attributed to a GGH-Ni(II) complex with water molecules coordinated to the bound metal. The precise chemical structure of such a complex is unknown. Both metallopeptide complexes are certainly in equilibrium with free GGH. However, the observed peak height of the latter species cannot provide quantitative information about the relative amount of noncomplexed peptide present in solution since the precise relationship between binding constants and the preservation of noncovalent complexes in the gas phase is not well established (*36*). The treatment of the peptide−nickel mixture with MMPP resulted in a significant decrease of the GGH-Ni(II) peak at 325.1 Da and the broadening of the peak around 352 Da (Figure 1C). Together, these two features suggest the extensive oxidative conversion of the GGH-Ni(II) complex into a novel species with a molecular mass near 352 Da. The latter derivative likely represents the proposed GGH-Ni(II)-oxo complex acting as the direct protein−protein cross-linker (*20*).

When the rigor F-actin−S-1 complex was subjected to oxidized GGH-Ni(II) and then analyzed by gel electrophoresis, a novel protein band pattern was obtained as depicted in Figure 2C. The reaction gave rise within a few seconds to a major product with an apparent molecular mass of 180 kDa and to a pair of closely migrating faint bands at the

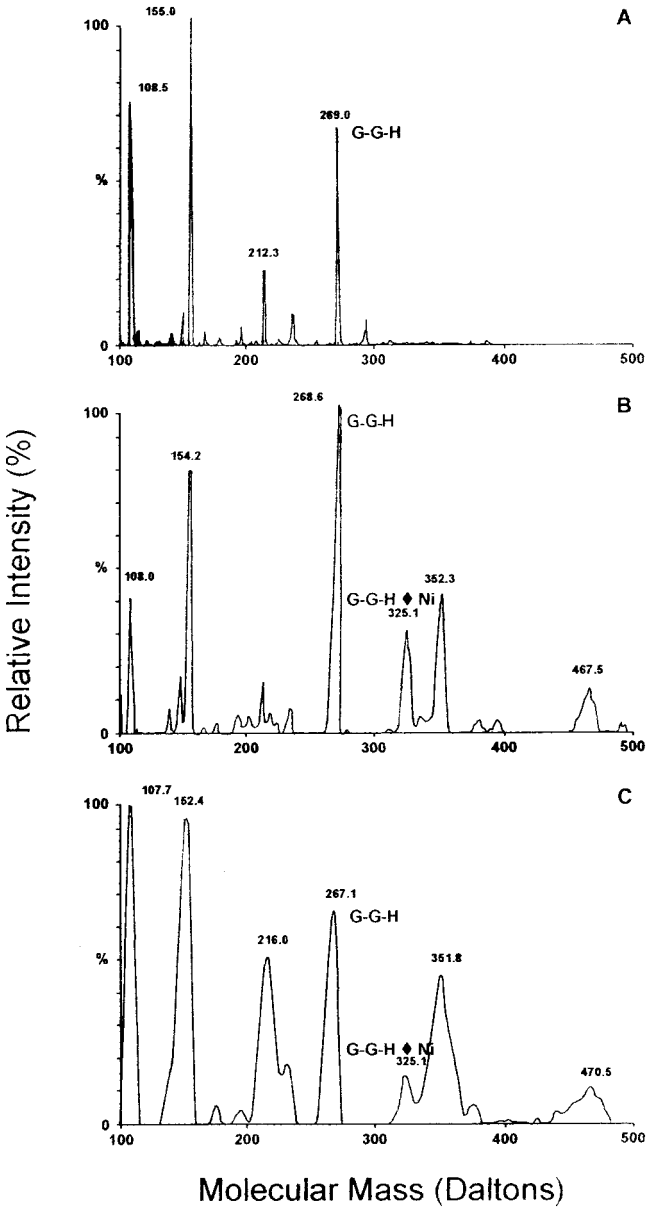

FIGURE 1: Electrospray ionization mass analysis of the cross-linking agent, GGH-Ni(II). The deconvoluted electrospray mass spectra are shown for the employed commercial sample of the free tripeptide GGH (A), its complex, GGH-Ni(II), obained by the addition of an equimolar amount of nickel acetate (B), and the oxidized GGH-Ni(II) form produced by further treatment with MMPP (C).

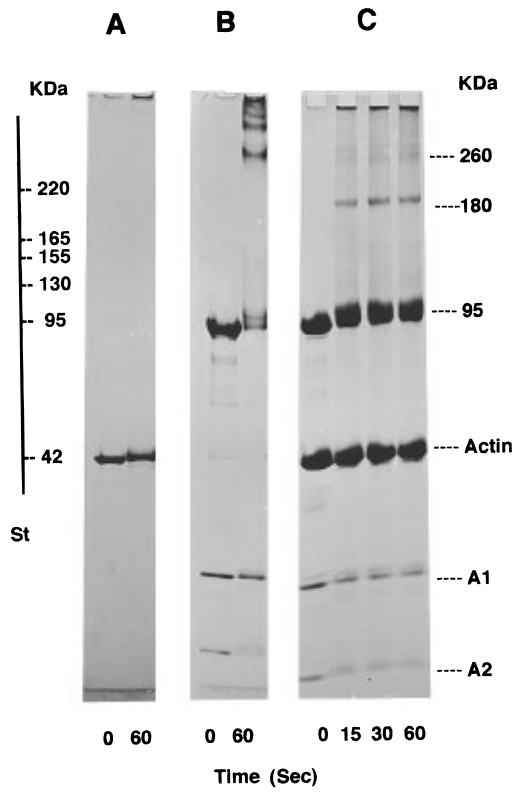

FIGURE 2: Electrophoretic analysis of the cross-linking between F-actin and S-1 with MMPP-oxidized GGH-Ni(II). Acto-S-1 (75 μM) in 50 mM Tris-HCl, 50 mM NaCl, and 2 mM $MgCl_2$ at pH 7.5 was cross-linked at 20 °C with GGH-Ni (1 mM) and MMPP (1 mM) as described in Materials and Methods. At the indicated time intervals of the chemical reaction, protein aliquots were directly mixed with Laemmli buffer containing 5% β-mercaptoethanol to quench the cross-linking process and then subjected to Na Dod SO_4 gel electrophoresis on a 5 to 18% gradient acrylamide (C). F-actin (40 μM) (A) and S-1 (40 μM) (B) were treated separately under similar conditions, as controls. St represents protein molecular weight markers.

260 kDa position. The former entity was not formed by incubating, under the same experimental conditions, actin or S-1, used separately as controls (panels A and B of Figure 2, respectively). While the electrophoretic pattern of actin did not change at all (Figure 2A), that of S-1 showed an accumulation of the 260 kDa bands together with a larger molecular mass species (Figure 2B). As will be demonstrated below, the 180 kDa entity is a conjugate of actin and the S-1 heavy chain whereas the 260 kDa materials represent cross-linked S-1 heavy chain oligomers, most likely dimers, generated only from the free S-1 which were suppressed or strongly diminished upon binding of S-1 to actin. Thus, the band intensity of the latter adducts is an intrinsic marker of the dissociation extent in solution of the acto-S-1 complex. As expected, no cross-linking event was observed by omitting one of the three reagents of the reaction or by replacing Ni-(II) with Cd, Co, or Zn. Similar acto-S-1 cross-linking patterns were obtained using actin:S-1 molar ratios of 1 or 2. Also, no change was noticed when the coupling process was conducted during a time period of longer than 1 min or when the pH was varied between 7.0 and 8.0. In contrast, the yield of the 180 kDa product, estimated by densitometry as approximately 8%, decreased with GGH-Ni(II) concentrations below 1 mM. However, it was not improved with higher reagent concentrations of up to 2 mM. The 1 min exposure of acto-S-1 to GGH-Ni(II) and MMPP did not induce any secondary oxidative cleavage of the S-1 or actin polypeptide chain (Figure 2). Moreover, and most importantly, all the residual non-cross-linked complex could be sedimented at the end of the reaction, indicating no apparent effect of the cross-linking compounds on the interaction properties of the reversibly associated proteins.

GGH-Ni(II) Cross-Linking of Acto-S-1 Complexed to Nucleotides or Nucleotide Analogs. Using the established optimal exprimental conditions, we further accomplished the cross-linking of acto-S-1 in the presence of MgATP, MgADP, or the nucleotide analogs $MgPP_i$, MgAMPPNP, or $MgADP{\cdot}AlF_4$. To ensure saturation of the complex with each ligand and a relatively high concentration of the corresponding ternary complex, the reactions were performed using increasing concentrations of nucleotide or analog which were added to 75 μM acto-S-1. The overall cross-linking analyses are presented in Figure 3. The inclusion of the

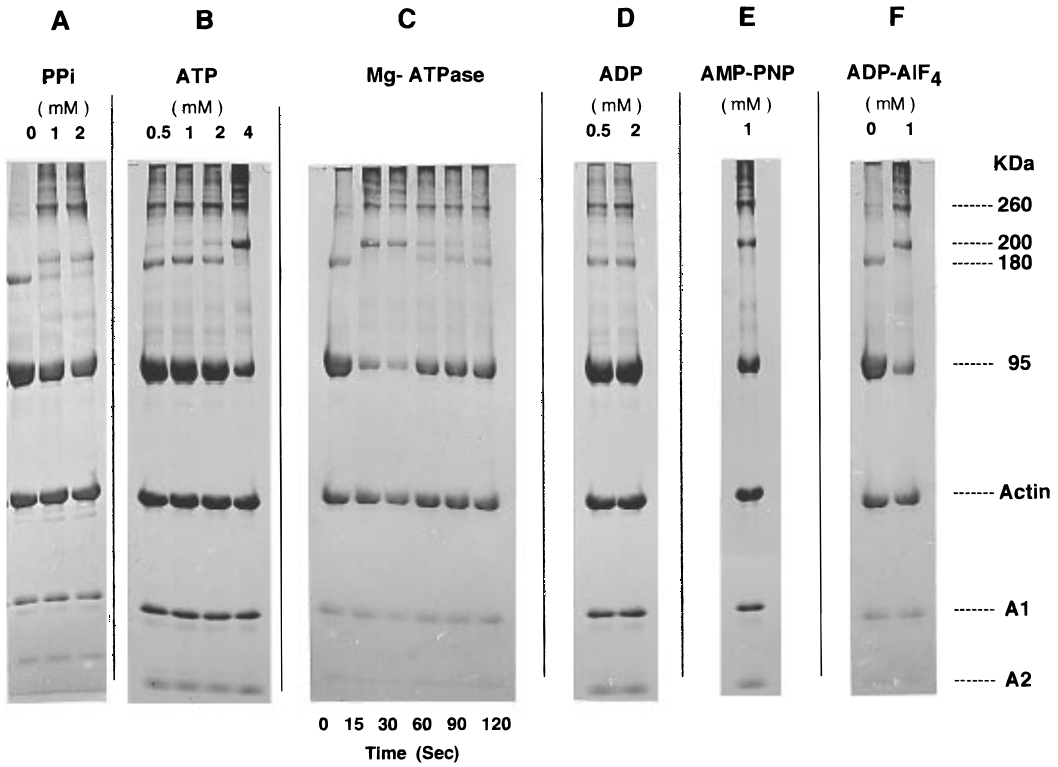

FIGURE 3: GGH-Ni(II) cross-linking of the acto-S-1 complex in the presence of nucleotides or nucleotide analogs and during the ATPase reaction. The cross-linking experiments were conducted for 45 s, as specified in Figure 2, using varying concentrations of $MgPP_i$ (A), MgATP (B), MgADP (D), MgAMPPNP (E), or Mg ADP·AlF_4 (F) which were added just before initiating the conjugation reaction with MMPP. The acto-S-1 complex (75 μM) was also incubated at 20 °C in 50 mM Tris-HCl, 50 mM NaCl, and 2 mM $MgCl_2$ at pH 7.5, with a fixed MgATP concentration of 4 mM; at the end of each indicated time interval of the ATPase reaction (0−120 s), the protein sample is immediately subjected to a 45 s cross-linking reaction (C). All cross-linking reactions were stopped with the Laemmli buffer and analyzed by 5 to 18% gradient acrylamide gel electrophoresis. In panels E and F, the gel profile at the optimal ligand concentration is shown.

γ-phosphate-containing ligands, PP_i, ATP, AMPPNP, and ADP·AlF_4 (panels A, B, E, and F of Figure 3, respectively), led to a typical change of the acto-S-1 cross-linking pattern. A novel protein component with an apparent molecular mass of 200 kDa was generated, and concomitantly, either the 180 kDa species disappeared, as observed with ATP, AMPPNP, and ADP·AlF_4 (panels B, E, and F of Figure 3, respectively), or its band intensity strongly decreased at the optimal ligand concentration employed, as in the case of PP_i (Figure 3A). In contrast, the cross-linking of the acto-S-1−ADP complex gave a prominent 180 kDa band together with a detectable minute amount of the 200 kDa product (Figure 3D). The latter material was never observed upon cross-linking the rigor acto-S-1. Because all nucleotides and analogs weaken the affinity of S-1 for actin, the formation of the 200 kDa material is accompanied by a greater production of the 260 kDa doublet issued form S-1 not attached to actin. Thus, each cross-linking pattern essentially reflects the rapid equilibrium in solution between the ternary acto-S-1−ligand complex and dissociated acto-S-1, under the experimental conditions used. Although nucleotides complexed to Ni(II) were reported to bind to the S-1 ATPase site (*38*), control experiments, employing such complexes and MMPP, but without GGH, failed to yield any cross-linked product. By densitometric scanning of the gels, we estimated the yield of the 200 kDa band mediated by GGH-Ni(II) to be 5−6%. Similar measurements for the acto-S-1−ADP complex provided an approximate value of the 180 kDa:200 kDa band ratio of 0.85:0.15(=5.6). For acto-S-1−PP_i, the value found was less than 0.1, whereas for the other complexes, the ratio was close to zero as there was no measurable 180 kDa band. Moreover, and most importantly, the high rate of the GGH-Ni(II)-induced cross-linking enabled us to monitor the relationship between the 180 and 200 kDa derivatives in the course of the acto-S-1 ATPase reaction (Figure 3C). For this purpose, a 45 s cross-linking was carried out on acto-S-1 incubated with a saturating concentration of ATP for varying time intervals between 0 and 120 s. During the first 30 s of the ATPase process, only the 200 kDa entity was produced. But, as the enzymatic reaction progressed and ATP was hydrolyzed, the band intensity of the latter species fell with a concomitant accumulation of the 180 kDa adduct. The final cross-linking pattern reached after 120 s of ATPase reaction was identical with that displayed by the acto-S-1−ADP complex (Figure 3D). A simple calculation based on the S-1 concentration (75 μM) and its activity of 1 s^{-1} at the beginning of the experiment indicated that about 4.5 μmol of ATP/min would be turned over and that upon 2 min of reaction all the ATP (4 mM) was consumed. Thus, the observed change in the migration pattern of the bands is correlated on the correct time scale to the ATPase intermediates. Collectively, the data suggest that the nucleotide-modulated generation of the 180 kDa−200 kDa protein complexes is a manifestation of the transition of acto-S-1 between the strongly attached state and the weakly attached state.

In order to determine the protein composition of the 180kDa−200 kDa bands, actin or S-1 was fluorescently labeled with monobromobimane prior to cross-linking. This fluorophor was selected because it did not react with the oxidized metal complex with severe quenching of the fluorescence in contrast to the class of dyes including an

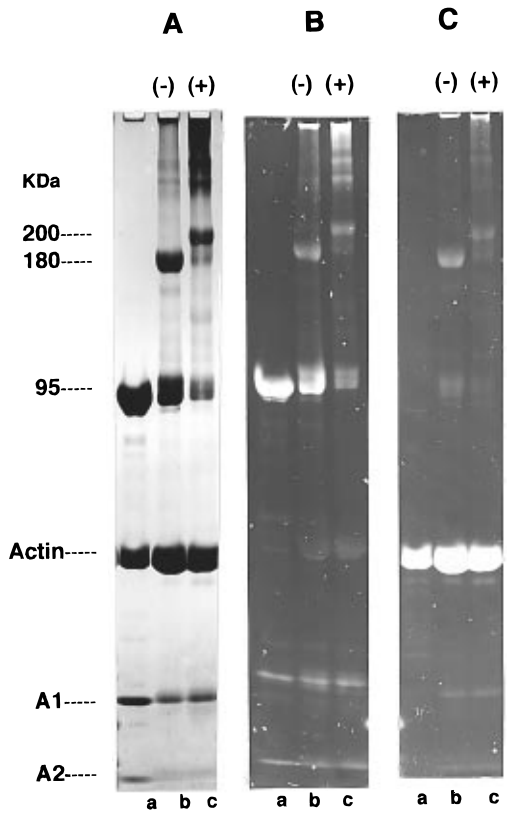

FIGURE 4: Determination of the protein composition of the 180 and 200 kDa covalent species. Oxidized GGH-Ni(II) was reacted for 1 min in the absence (−) or presence (+) of 1 mM $MgPP_i$ with acto-S-1 complexes (50 μM), including either bimane-labeled S-1 (B) or bimane-labeled actin (C), using the experimental conditions reported in Figure 2. After quenching of the cross-linking with β-mercaptoethanol added at a 100-fold molar excess over MMPP, the protein mixtures were supplemented with an equal volume of dissociating solution and centrifuged as specified in Materials and Methods. The corresponding pellets were resuspended in 50 mM MOPS and 2 mM $MgCl_2$ at pH 7.0 and analyzed by gel electrophoresis. The fluorescence incorporation into the 180 and 200 kDa adducts (lanes b and c, respectively) was evaluated after the gels were viewed under UV light (B and C) prior to Coomassie blue staining (A). Lanes a are acto-S-1 complexes before cross-linking.

aromatic group. As shown in lanes b and c of Figure 4B, both adducts incorporated the fluorescence of the bimane−S-1 heavy chain as well as the bimane−actin fluorescence (Figure 4C, lanes b and c), indicating unambiguously that they result from the covalent coupling of actin to the S-1 heavy chain. On the other hand, only the fluorescence of the bimane−S-1 heavy chain was associated with the slower migrating species with a mass value of 260 kDa, thus substantiating their identification as cross-linked heavy chain oligomers (Figure 4B, lane c).

Finally, we have also analyzed the elevated Mg^{2+}-ATPase activity displayed by the covalent acto-S-1 complexes corresponding to the 180 or 200 kDa entities. The measured turnover rates were 20 and 4.5 s^{-1}, respectively. The ATPase rate of the former complex compares well with that previously found for acto-S-1 complexes cross-linked with different cross-linkers (*17*). The lower enzymatic activity of the complex related to the 200 kDa species was brought about by secondary oxidative effects of the cross-linking reaction on S-1 which became less tightly bound to and protected by actin in the presence of the γ-phosphate-containing ligands. Indeed, control actin-activated ATPase determinations on the respective residual un-cross-linked S-1 species also gave the different turnover rate values of 0.6 and 0.15 s^{-1}, respectively.

Identification of the GGH-Ni(II)-Cross-Linked Fragments on the S-1 Heavy Chain. To characterize the S-1 heavy chain regions cross-linked to actin, the cross-linking reactions with or without nucleotides or analogs were performed on complexes of F-actin and preformed proteolytic S-1 derivatives (25−50−20 kDa)-S-1 (Figure 5A) or (28−48−22 kDa)-S-1 (Figure 5B). These complexes included either fluorescent actin or fluorescent fragmented S-1. The rigor complex between actin and the tryptic (25−50−20 kDa)-S-1 produced a single 90 kDa band containing the actin fluorescence only (Figure 5A, lanes b and f) and reacting with the antibody against the 50 kDa heavy chain fragment (Figure 5A, lane h). This product was regarded as the actin−50 kDa fragment species derived from the 180 kDa conjugate. The cross-linking of the same complex in the presence of $MgPP_i$ yielded a single slower band including also the actin fluorescence only and which obviously represents the actin−50 kDa peptide adduct related to the nucleotide-dependent 200 kDa species (Figure 5A, lanes c and g). When the S-1 derivative employed is the V8-split (28−48−22 kDa)-S-1, the fluorescence patterns indicated the similar formation of two differently migrating actin−48 kDa peptide bands (Figure 5B, lanes b−g). In addition, each species was accompanied by the production of a new less abundant protein band which was associated with the fluorescence of actin and the fluorescence of the 22 kDa S-1 heavy chain fragment (Figure 5B, lanes b−g). It should represent an actin−22 kDa S-1 heavy chain adduct. Notably, the generation of this peptide material was negligible during the coupling of actin to the tryptic S-1 (Figure 5A), suggesting that the structural integrity of the 50−20 kDa connector junction, present in the 22 kDa fragment but absent in the 20 kDa peptide, is required for cross-linking. From all these data, we conclude that GGH-Ni(II) promotes the cross-linking of actin mainly to the central 50 kDa and marginally to the COOH-terminal 22 kDa segments of the S-1 heavy chain. The former cross-linking event appears to be particularly sensitive to nucleotide binding to S-1 and determines the above observed change in the electrophoretic mobility of the covalent actin−95 kDa S-1 heavy chain complex. The latter peculiarity is unlikely to result from an internal cross-linking in actin and/or the S-1 heavy chain as the residual proteins migrated normally. Finally, the complete lack of interfragment cross-linking clearly indicates that the intermolecular coupling between actin and the S-1 heavy chain was the major process catalyzed by oxidized GGH-Ni(II).

Characterization of the Cross-Linked Peptide Stretches in Actin and in the 50 kDa Heavy Chain Segment. In order to specify the site(s) of cross-linking between actin and the 50 kDa region, we combined two experimental approaches. The first one involved the coupling of S-1 to two different subtilisin-cleaved F-actin derivatives and the cross-linking of F-actin to the tryptic (25−40−31 kDa)-S-1. The second approach was based on the specific proteolytic digestion of either actin or the 50 kDa heavy chain region within the preformed covalent acto-S-1 complexes. The overall results are depicted in Figures 6 and 7. The reaction of GGH-Ni-(II) with the rigor complex of S-1 and polymerized subtilisin-split (9−35 kDa)-actin generated a single new product with a mass value of 170 kDa which was replaced by a 195 kDa

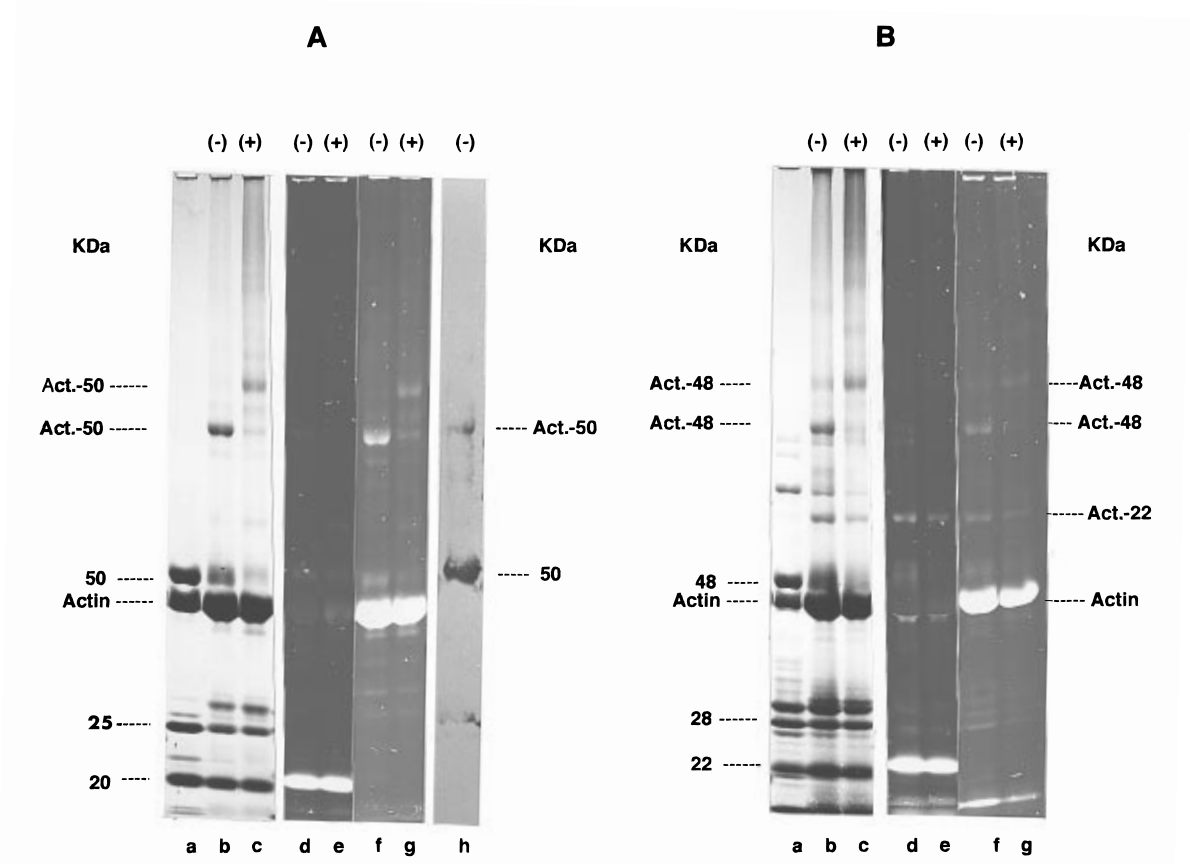

FIGURE 5: Analysis of the cross-linking between F-actin and proteolytic S-1 derivatives with oxidized GGH-Ni(II). Complexes at 50 μM of actin and (25−50−20 kDa)-S-1 (A) or (28−48−22 kDa)-S-1 (B) were cross-linked for 1 min in the absence (−) or in the presence (+) of 1 mM $MgPP_i$, and at the end of the reaction, they were processed as in Figure 4. They comprised either fluorescent bimane−S-1 (lanes d and e) or fluorescent bimane−actin (lanes f and g). Coomassie blue-stained 5 to 18% acrylamide gels (lanes a−c) were compared with corresponding fluorescent gels (lanes d−g) viewed under UV light. The gel of the actin−(25−50−20 kDa)-S-1 complex cross-linked without $MgPP_i$ was also stained with the antipeptide antibody recognizing the 50 kDa heavy chain segment to visualize the actin−50 kDa adduct (A, lane h).

species when $MgPP_i$ was present in the cross-linking solution (Figure 6A, lanes a and b, respectively). They could be only the adducts of the S-1 heavy chain and the 35 kDa COOH-terminal actin fragment spanning residues 48−375. For the two same reactions performed on the complex of S-1 and subtilisin-cut (27−16 kDa)-F-actin−ADP·BeF_x, the two new distinct entities detected displayed apparent molecular mass values of 150 and 160 kDa, respectively (Figure 6B, lanes b and c). They were thought to represent the two cross-linked complexes of the S-1 heavy chain and the 27 kDa NH_2-terminal actin fragment encompasssing amino acids 1−234. On the other hand, the direct thrombic digestion of the two preformed covalent acto-S-1 complexes, including the 180 or 200 kDa actin−heavy chain conjugates, resulted also in the production of two new protein bands with molecular masses of 110 kDa and 115 kDa, respectively (Figure 6C, lanes b and d). They were regarded as the adducts of the intact S-1 heavy chain and the 10 kDa actin fragment consisting of residues 40−113. This assignment was confirmed by immunoblotting of the 115 kDa species (Figure 6C, lane e) and the 110 kDa band (data not shown) with the antibody to the 40−113 actin segment. On the basis of these combined data, which are summarized in Figure 8, we conclude that the stretch of actin between Gly 48 and Lys 113 harbors the site(s) involved in its cross-linking to the S-1 heavy chain in the absence as well as in the presence of nucleotides or analogs.

Finally, the location of the cross-linking site(s) within the 50 kDa heavy chain fragment was assessed by first cross-linking the rigor complex of F-actin and the tryptic (25−40−31 kDa)-S-1 derivative. A moderate amount of the latter material could be reproducibly generated by digesting the native F-actin−S-1 complex at a high S-1:protease weight ratio (Figure 7A, lane a). Actin afforded protection against the scission of the 50−20 kDa junction, giving rise to an accumulation of intact COOH-terminal 70 kDa heavy chain fragment, but it also induced a selective partial cleavage of the latter segment into fragments of 40 and 31 kDa. By sequencing the 10 NH_2-terminal amino acids of the isolated 31 kDa peptide, we identified its NH_2 terminus as Ser 562. The proteolytic sensitivity of the heavy chain at this site has been described earlier (24). Following gel electrophoresis of the GGH-Ni(II)-treated acto-S-1 digest (Figure 7A, lane b), the nature of the heavy chain fragments cross-linked to actin was probed by the use of the antipeptide antibody specifically recognizing the 17-residue segment including Arg 405 in the 50 kDa region of the skeletal S-1 heavy chain (Figure 7A, lane c). Besides the expected actin−70 kDa and actin−50 kDa adducts, the immunoblot revealed also a new faster migrating band which must correspond to the covalent complex of actin and the 40 kDa fragment spanning residues 214−561. The fluorescence pattern obtained when the same experiment was performed using the fragmented bimane−S-1 confirmed this assignment as no product issued from the cross-linking of actin to fluorescent 31 kDa peptide was detected (data not shown).

To further narrow the positioning of the heavy chain cross-links, the preformed covalent complex between F-actin and

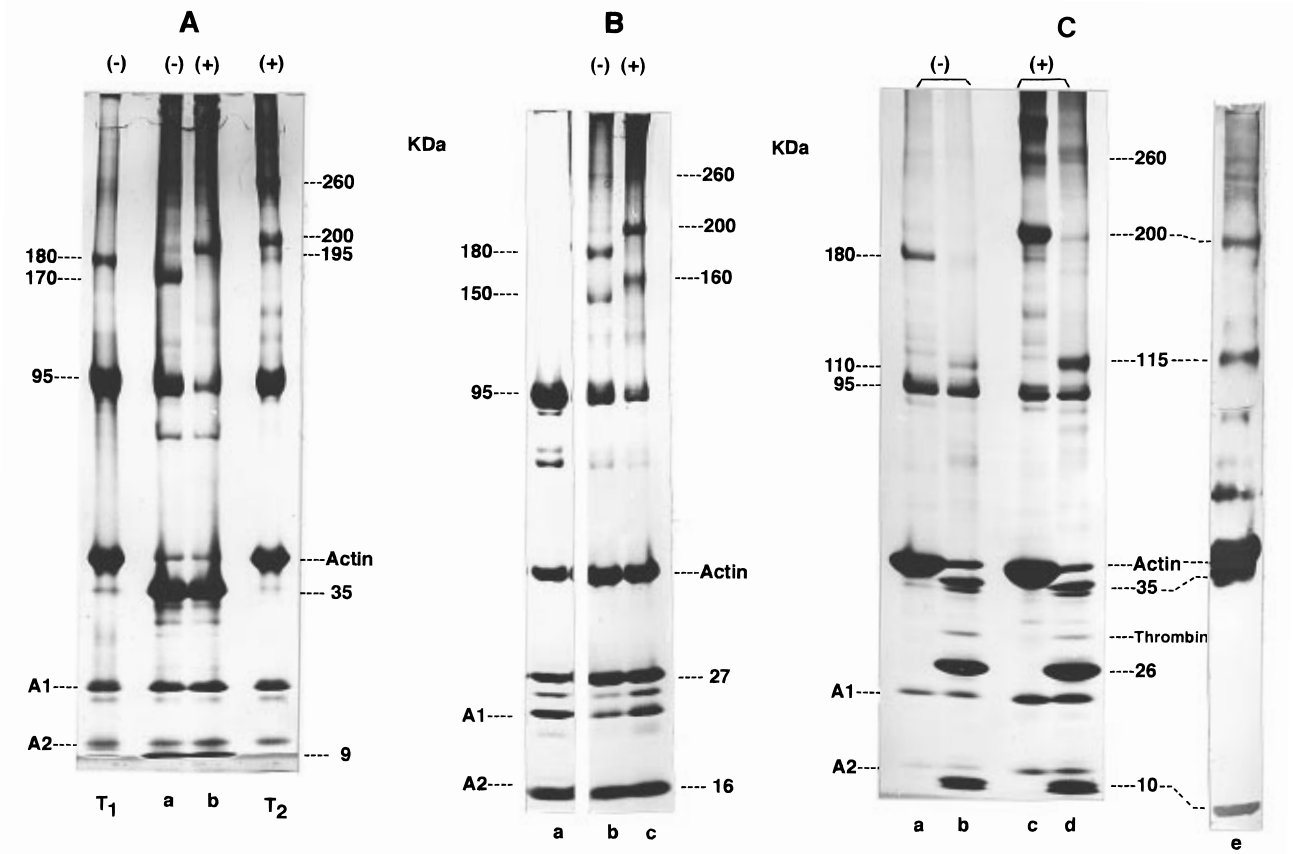

FIGURE 6: Identification of the cross-linked actin segment. (A) S-1 (60 μM) was coupled for 1 min at 20 °C to polymerized subtilisin−G-actin (60 μM) with oxidized GGH-Ni(II), in the absence (−) (lane a) or presence (+) (lane b) of 2 mM $MgPP_i$. The protein mixtures were traited with β-mercaptoethanol followed by the dissociating solution and then centrifuged as detailed in Figure 4. The resupended protein pellets were electrophoresed. Cross-linked acto-S-1 (T1) and acto-S-1−$MgPP_i$ (T2) complexes were used as controls. (B) S-1 was similarly cross-linked to subtilisin-split MgADP·BeF_x-F-actin with (lane c) or without (lane b) added $MgPP_i$. Lane a is a gel pattern of the complex of S-1 and the proteolytic F-actin derivative before cross-linking. (C) Thrombic cleavage of the 180 kDa (lanes a and b) and 200 kDa (lanes c and d) covalent species generated by GGH-Ni(II) cross-linking of the acto-S-1 complex in the absence (−) and presence (+) of $MgPP_i$, respectively. The cross-linked F-actin−S-1 complexes obtained after 1 min of conjugation reaction were isolated, depolymerized, and digested with thrombin as indicated in Materials and Methods. The Coomassie blue-stained gel profiles before (lanes a and c) and after (lanes b and d) the proteolysis are shown. Lane e is an immunoblot of the digest of the 200 kDa derivative using the antibody to the actin segment 40−113. Note that the digest of the 180 kDa product gave an identical immunostaining pattern.

(25−50−20 kDa)-S-1 was subjected to an extensive tryptic hydrolysis under dissociating conditions. The electropherogram of the digest, presented in lanes a and b of Figure 7B, showed a decrease of the band intensity of the initial actin−50 kDa fragment adduct with a concomitant production of a new species migrating at the 60 kDa position. This protein band was stained by two distinct actin antibodies, one directed to the NH_2 terminus (Figure 7B, lanes c and d) and the other to the COOH terminus of actin (data not shown). On the other hand, it did not react with the antibody against the heavy chain stretch around Arg 405 (data not shown). Amino acid sequencing of the isolated 60 kDa band revealed a single NH_2-terminal sequence begining at Glu 506 of the S-1 heavy chain. This result in conjunction with the Western blotting indicates that it was composed of intact actin and, most likely, the COOH-terminal portion of the 50 kDa region between residues 506 and 636. From the overall data schematically depicted Figure 8, it can be deduced that the cross-linking site(s) to actin on the 50 kDa fragment resides within the strand encompassing Glu 506−Lys 561. It is noteworthy that the slower actin−50 kDa fragment adduct induced by the phosphorylated ligands did also generate, upon extensive tryptic hydrolysis, a slower species with an apparent mass of 65 kDa (data not shown). Although we have not analyzed it in more detail, we anticipate that its protein composition is similar to that found for the 60 kDa derivative and, therefore, that the 506−561 segment is also engaged in the cross-linking to actin modulated by nucleotides or analogs.

DISCUSSION

In the present work, we have designed experimental conditions allowing nucleotide-modulated cross-linking of F-actin to the 95 kDa S-1 heavy chain with the oxidized GGH-Ni(II) chelate. Except for the production of heavy chain oligomers from S-1 not attached to actin, neither actin−actin nor heavy chain−light chain coupling occurred to a significant extent. The former intermolecular cross-linking between S-1 molecules could result from an autoassociation of the protein caused by the oxidation with MMPP of sensitive thiols such as SH1 and SH2. The latter sulfhydryls are known to be protected from chemical modification by rigor binding of S-1 to F-actin (*39*) which also protected the S-1 against ATPase loss during the GGH-Ni(II)-mediated cross-linking reaction.

In the two covalent actin−S-1 heavy chain complexes of 180 and 200 kDa we have characterized, actin was conjugated mainly to the 50 kDa heavy chain segment which harbors most of the structural elements contributing to the interface between F-actin and S-1 (*10, 11*). A striking feature

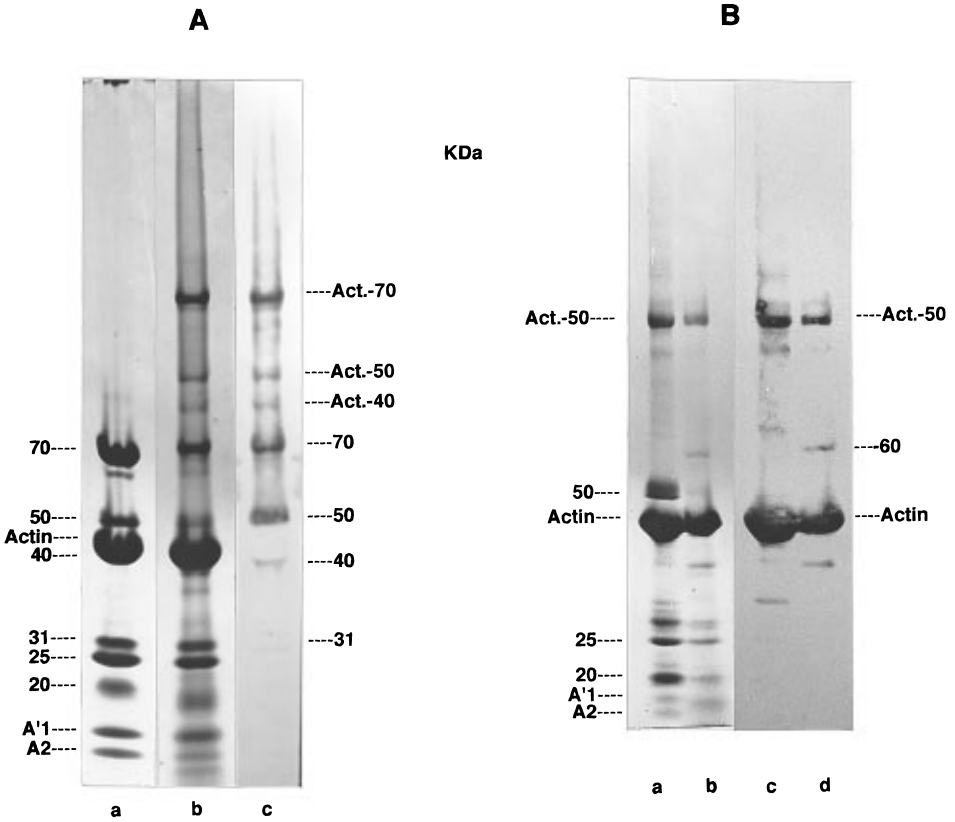

FIGURE 7: Identification of the cross-linked region within the 50 kDa S-1 heavy chain fragment. (A) The complex of F-actin and the tryptic (25−40−31 kDa)-S-1 derivative (lane a) (75 μM) was cross-linked with oxidized GGH-Ni(II) for 1 min. After the quenching of the reaction with β-mercaptoehtanol and centrifugation in the presence of the dissociating solution, the pelleted proteins were analyzed by gel electrophoresis. The Coomassie blue-stained protein band pattern (lane b) was compared with the corresponding immunoblot (lane c) using the anti-50 kDa fragment antibody. (B) The complex of F-actin and (25−50−20 kDa)-S-1 (75 μM) was cross-linked for 1 min, treated with β-mercaptoethanol, mixed with an equal volume of dissociating solution, and directly subjected to extensive tryptic hydrolysis as specified in Materials and Methods. Cross-linked protein samples were analyzed by gel electrophoresis before (lanes a and c) and after tryptic digestion (lanes b and d). The gels were stained with Coomassie blue (lanes a and b) or immunoblotted with anti-actin antibodies directed against residues 1−12 (lanes c and d). Note that an identical immunoblot was obtained using antibodies directed to the 11 C-terminal actin residues.

of the actin−50 kDa fragment adduct was the change of its hydrodynamic properties on the electrophoretic gels upon association of a γ-phosphate-containing nucleotide or analog to the S-1 ATPase site during the acto-S-1 coupling process. No such nucleotide-dependent alteration of the electrophoretic mobility was previously observed for the covalent actin−50 kDa peptide complexes generated by acto-S-1 cross-linking *via* polar residues of the interface (*17, 40*−*42*). The acto-S-1 cross-linking patterns we obtained for the first time in this study can be best interpreted in terms of the three-step mechanism of the actomyosin interaction in solution which involves a nucleotide-dependent equilibrium between two conformationally different states designated the A state and the R state (*2, 3*). The first complex, consisting of weakly attached acto-S-1, predominantly formed upon binding of the γ-phosphate-containing ligands, ATP, PP_i, AMPPPNP, or ADP·AlF_4, was trapped by GGH-Ni(II) cross-linking as a covalent 200 kDa species. The second complex including strongly attached acto-S-1, accumulated in the absence of nucleotides or with ADP bound, was cross-linked as a 180 kDa entity. This proposal is supported by the correlation between the reported equilibrium constants K_2 for the A to R isomerization states of acto-S-1 and the band ratios we measured for the 180 and 200 kDa covalent complexes (Table 1). It is reinforced by the finding that the acto-S-1−ADP and acto-S-1−PP_i complexes, which were predicted to be able to occupy both states, have also generated the pair of 180 and 200 kDa species. Furthermore, the measured relative amounts of the two latter covalent products were as expected from the reported values of the equilibrium constant K_2 defining for the acto-S-1−ADP and acto-S-1−PP_i complexes the fraction of each complex in the two states A and R (*2, 43, 44*). Earlier, the detection in solution of these two major acto-S-1 complexes and the analysis of their interconversion were achieved using fluorescence spectroscopy with either protein labeled with an extrinsic fluorophor. The cross-linking of native acto-S-1 with oxidized GGH-Ni(II) offers a novel useful tool for monitoring these complexes under a variety of experimental conditions as long as they do not interfere with the production of the protein-derived aromatic radicals.

The GGH-Ni(II)-catalyzed acto-S-1 conjugation is assumed to be initiated by the radicalization of the aromatic group of phenylalanine, tyrosine, or tryptophan residues which could be placed on actin or S-1. This step would be followed by the direct addition of the transient reactive free radical species to the adjacent double bond of either another aromatic ring or the carbonyl function of the polypeptide chain (*20*). The efficiency of the overall reaction is thought to be dependent on the number and degree of exposure of the aromatic side chains at the protein complex interface. The estimated efficiency of the acto-S-1 cross-linking in the presence of the γ-phosphate-containing ligands is close to that found with the rigor complex when only the amount of

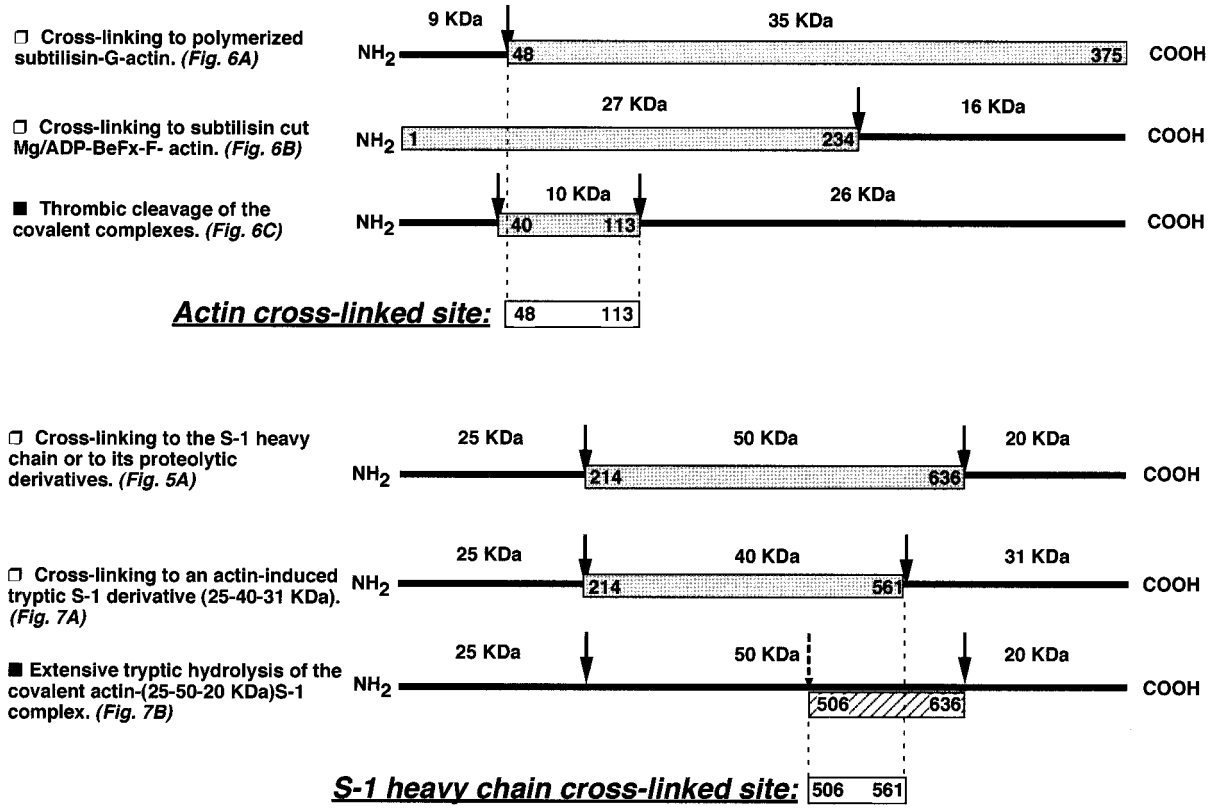

FIGURE 8: Schematic diagram of the localization of the GGH-Ni(II)-cross-linked segments along the actin and the 50 kDa S-1 heavy chain sequences. The positioning of the smallest peptide stretch including the cross-links of actin (Gly 48−Lys 113) or the 50 kDa fragment (Glu 506−Lys 561) was deduced by combining the data from the proteolytic cleavage of the covalent acto-S-1 complexes (■) with those of the direct cross-linking reactions between S-1 and proteolytic F-actin derivatives or between F-actin and proteolytic S-1 derivatives (□). Arrows indicate the proteolytic sites. Shaded bars represent the cross-linked actin or S-1 heavy chain fragments. Solid bars refer to the actin or S-1 heavy chain segments not involved in the cross-linking. The dashed arrow is the site of tryptic cleavage yielding the 60 kDa adduct consisting of actin and the heavy chain segment 506−636 (hatched bar).

Table 1: Correlation between the Equilibrium Constants (K_2) Reported for the A (Weak) to R (Strong) Isomerization States of Acto-S-1 and the Band Ratios Measured for the GGH-Ni(II)-Induced 180−200 kDa Covalent Complexes

bound nucleotide or analog	K_2 ([R]/[A])[a]	[180 kDa]:[200 kDa] band ratio[b]
ATP	<0.01	~0
PP_i	2.3[c]	0.1
AMP·PNP	0.1	~0
ADP	10	6
ADP·Vi (ADP·AlF_4)[d]	<0.01	~0
no ligand[e]	−	−

[a] From the studies in refs 2, 43, and 44. [b] Determined by densitometry as described in Materials and Methods. [c] This K_2 value is given as a maximum value which could be subject to a large error due to a possible overestimation of the amount of complex in the R state in the presence of PP_i (*44*). [d] The transition state analog used in the present study. [e] No trace of the 200 kDa product was noticed as expected from the reported K_2 value of 300.

associated and therefore cross-linkable acto-S-1 was taken into consideration. Also in both cases, the 50 and 22 kDa fragments contributed to the observed cross-linking of the S-1 heavy chain with actin. These features suggest little difference in the number and/or solvent accessibility of the aromatic constituents participating in the cross-linking of the weak and strong acto-S-1 complexes. However, the latter apolar components may be functionally important in acto-S-1 weak binding during the ATPase cycle. This proposal is consistent with results indicating that the electrostatic contacts between the NH_2-terminal actin segment of residues 1−28 and the S-1 heavy chain loop of amino acids 626−647, while involved in the actin activation of the S-1 ATPase, do not seem to be the main determinants of the strength of the actin-S-1 bond in the presence of ATP (*42*, *45*, *46*). It is also in accordance with the suggested association of a stereospecific interaction involving hydrophobic residues with the weak A state (*8*).

The location of the S-1 heavy chain cross-linking site(s) between residues 506 and 561 is of particular interest as this segment makes up part of the lower subdomain of the 50 kDa region (Figure 9) and includes the helix−loop−helix motif of Gly 516−His 558 which was proposed to represent the primary, stereospecific, and hydrophobic actin-binding site of S-1 (*10*, *11*). According to the structural models of acto-S-1 with various bound nucleotide and transition state analogs, the lower 50 kDa subdomain would play a major role in the molecular mechanism of energy transduction (*47*−*50*). During the acto-S-1 ATPase cycle, it specifically communicates with the γ-phosphate binding subsite and undergoes movements which cause substantial alterations in both the nucleotide binding region and the actin-binding interface. The conformational change of the latter region, thought to be important for modulating the actin binding affinity of S-1, might have induced the observed shift of the electrophoretic mobility of the covalent actin−50 kDa fragment complex by modifying the nature of the juxtaposed sites cross-linked by GGH-Ni(II) and/or the folding of the cross-linked peptide stretches. In this regard, chemical cross-linking is known to have the potential not only for detecting protein−protein interactions but also for probing polypeptide

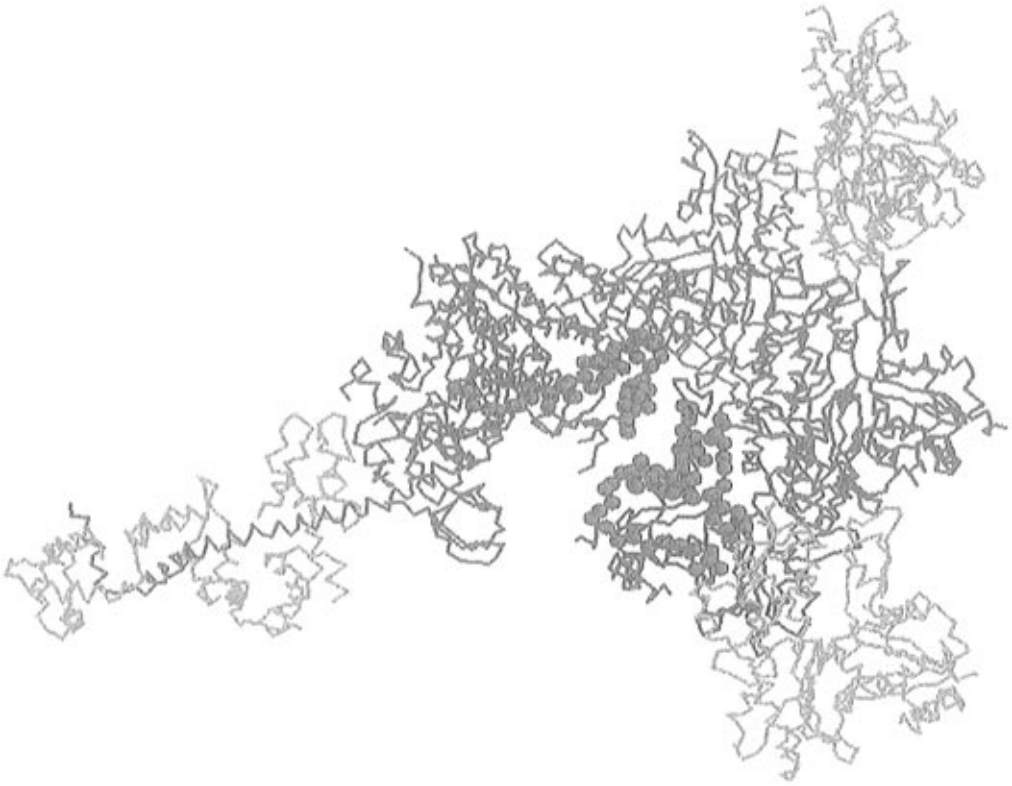

FIGURE 9: Relative location of the cross-linked peptide stretches in the atomic model of the acto-S-1 complex. The identified segment of residues 48−113 in the lower actin monomer is represented by blue spheres, and the identified peptide of residues 506−561 in the lower 50 kDa subdomain of the S-1 bound to the upper actin monomer is represented by orange spheres. The α-carbon coordinates of the acto-S-1 complex were kindly supplied by I. Rayment.

chain conformation (*51*, *52*). The complementary actin segment we have identified encompasses amino acids 48−113. It overlaps the outer edge of subdomain 2 and the α-helical top of subdomain 1 in actin. Several proteolytic reactions we have attempted to shorten this stretch and further characterize the cross-linked residue(s) have failed owing to a strong protective effect of the covalently linked S-1. However, the relative location of the two cross-linked acto-S-1 fragments in the atomic model of the rigor acto-S-1 complex reveals that the S-1 bound to the primary actin monomer has been cross-linked to the adjacent lower actin monomer (Figure 9). Also, in this model, the C-terminal helix (Asp 547−His 558) of the strong hydrophobic actin-binding motif of S-1 is in close proximity to the outer part of subdomain 2 of the actin below. Earlier, using two different cross-linking agents with a 9 Å span, we have shown the cross-linking of the actin segment 48−67, *via* Lys 50, to the central 48 kDa fragment of the S-1 heavy chain (*19*, *53*). More recently, we have described the selective substitution of Lys 553 in S-1 with a fluorescein derivative in an actin-sensitive manner (*28*). Thus, it is conceivable that the GGH-Ni(II)-mediated cross-links could be established between the region around Lys 50 of actin and the nearby helical S-1 heavy chain strand 547−558.

Protein−protein cross-linking with the oxidized GGH-Ni-(II) agent was first analyzed with the use of protein complexes of unknown molecular structure (*20*). The application of the reaction to the acto-S-1 complex whose atomic model is available offered the opportunity to further assess the specificity of this novel cross-linking approach. The predominant cross-linking events we observed took place in the heavy chain segment of residues 506−561, part of which is known to be directly implicated in the acto-S-1 interactions. The final identification of the cross-linked residues will help to provide a firm basis for the putative chemistry of the coupling process. The apparent site specificity of the reaction in conjunction with the sensitivity of the cross-linking pattern to the binding of nucleotides and analogs, makes the GGH-Ni(II) cross-linking potentially suitable for probing other unknown protein motor-based complexes such as the kinesin or ncd-microtubules system which also switches from weak to strong binding *via* ADP release (*54*) and where the nature and dynamics of the hydrophobic recognition components of the complex remain to be elucidated.

ACKNOWLEDGMENT

We thank Dr. B. Calas for help in the mass spectrometric analyses.

REFERENCES

1. Greene, L. E., and Eisenberg, E. (1980) *J. Biol. Chem. 255*, 549−554.
2. Geeves, M. A. (1991) *Biochem. J. 274*, 1−14.
3. Geeves, M. A., and Conibear, P. B. (1995) *Biophys. J. 68*, 194s−201s.
4. Franks-Skiba, K., and Cooke, R. (1995) *Biophys. J. 68*, 142s−149s.
5. Murphy, K. P., Zhao, Y., and Kawai, M. (1996) *J. Exp. Biol. 199*, 2565−2571.
6. Luo, Y., Wang, D., Cremo, C. R., Pate, E., Cooke, R., and Yount, R. (1995) *Biochemistry 34*, 1978−1987.
7. Lehman, W., Craig, R., and Vibert, P. (1994) *Nature 368*, 65−67.
8. Holmes, K. C. (1995) *Biophys. J. 68*, 2s−7s.

9. Lehman, W., Vibert, P., Uman, P., and Craig, R. (1995) *J. Mol. Biol. 251*, 191−196.
10. Rayment, I., Holden, H. M., Whittaker, M., Yohn, C. B., Lorenz, M., Holmes, K. C., and Milligan, R. A. (1993) *Science 261*, 58−65.
11. Schroder, R. R., Manstein, D. J., Jahn, W., Holden, H., Rayment, I., Homes, K. C., and Spudich, J. A. (1993) *Nature 364*, 171−174.
12. Miller, C. J., Doyle, T. C., Bobkova, E., Botstein, D., and Reisler, E. (1996) *Biochemistry 35*, 3670−3676.
13. Onishi, H., Morales, M. F., Katoh, K., and Fujiwara, K. (1995) *Proc. Natl. Acad. Sci. U.S.A. 92*, 11965−11969.
14. Mornet, D., Bertrand, R., Pantel, P., Audemard, E., and Kassab, R. (1981) *Nature 292*, 301−306.
15. Labbé, J. P., Mornet, D., Roseau, G., and Kassab, R. (1982) *Biochemistry 21*, 6897−6902.
16. Sutoh, K. (1982) *Biochemistry 21*, 3654−3661.
17. Bertrand, R., Chaussepied, P., Kassab, R., Boyer, M., Roustan, C., and Benyamin, Y. (1988) *Biochemistry 27*, 5728−5736.
18. Bonafé, N., Chaussepied, P., Capony, J. P., Derancourt, J., and Kassab, R. (1993) *Eur. J. Biochem. 181*, 747−754.
19. Bonafé, N., Mathieu, M., Kassab, R., and Chaussepied, P. (1994) *Biochemistry 33*, 2594−2603.
20. Brown, K. C., Yang, S.-H., and Kodadek, T. (1995) *Biochemistry 34*, 4733−4739.
21. Bertrand, R., and Kassab, R. (1996) *Biophys. J. 70*, 159a.
22. Offer, G., Moss, C., and Starr, R. (1973) *J. Mol. Biol. 74*, 653−679.
23. Weeds, A. G., and Taylor, R. S. (1975) *Nature 257*, 54−56.
24. Chaussepied, P., Mornet, D., Audemard, E., Derancourt, J., and Kassab, R. (1986) *Biochemistry 25*, 1134−1140.
25. Eisenberg, E., and Kielley, W. W. (1974) *J. Biol. Chem. 249*, 4742−4748.
26. Kasprzak, A. A., Takashi, R., and Morales, M. F. (1988) *Biochemistry 27*, 4512−4522.
27. Mornet, D., Ue, K., and Morales, M. F. (1985) *Proc. Natl. Acad. Sci. U.S.A. 82*, 1658−1662.
28. Bertrand, R., Derancourt, J., and Kassab, R. (1995) *Biochemistry 34*, 9500−9507.
29. Kiessling, P., Jahn, W., Maier, G., Polzar, B., and Mannherz, H. G. (1995) *Biochemistry 34*, 14834−14842.
30. Vahdat, A., Miller, C., Phillips, M., Muhlrad, A., and Reisler, E. (1995) *FEBS Lett. 365*, 149−151.
31. Polzar, B., Rösch, A., and Mannherz, H. G. (1989) *Eur. J. Cell Biol. 50*, 220−229.
32. Bonafé, N., and Chaussepied, P. (1995) *Biophys. J. 68*, 35s−43s.
33. Towbin, H., Stoehelin, T., and Gordon, J. (1979) *Proc. Natl. Acad. Sci. U.S.A. 76*, 4350−4354.
34. Mornet, D., Pantel, P., Audemard, E. and Kassab, R. (1979) *Eur. J. Biochem. 100*, 421−431.
35. Laffite, D., Capony, J. P., Grassy, G., Haiech, J., and Calas, B. (1995) *Biochemistry 34*, 13825−13832.
36. Smith, R. D., and Light-Wahl, K. J. (1993) *Biol. Mass Spectrom. 22*, 493−501.
37. Loo, J. A. (1995) *Bioconjugate Chem. 6*, 644−665.
38. Peyser, Y. M., Ben-Hur, M., Weber, M. M., and Muhlrad, A. (1996) *Biochemistry 35*, 4409−4416.
39. Duke, J., Takashi, R., Ue, K., and Morales, M. F. (1976) *Proc. Natl. Acad. Sci. U.S.A. 73*, 302−306.
40. Chen, T., Applegate, D., and Reisler, E. (1985) *Biochemistry 24*, 137−144.
41. Arata, T. (1986) *J. Mol. Biol. 191*, 107−116.
42. Yamamoto, K. (1989) *Biochemistry 28*, 5573−5577.
43. Geeves, M. A., Goody, R. S., and Gutfreund, H. (1984) *J. Muscle Res. Cell Motil. 5*, 351−361.
44. Geeves, M. A., and Jeffries, T. F. (1988) *Biochem. J. 256*, 41−46.
45. Cheung, P., and Reisler, E. (1992) *Biochem. Biophys. Res. Commun. 189*, 1143−1149.
46. Kunori, S., Katoh, T., Mogi, Y., and Morita, F. (1995) *J. Biochem.* (Tokyo) *118*, 1239−1247.
47. Fisher, A. J., Smith, C. A., Thoden, J. B., Smith, R., Sutoh, K., Holden, H. M., and Rayment, I. (1995) *Biochemistry 34*, 8960−8972.
48. Smith, C. A., and Rayment, I. (1995) *Biochemistry 34*, 8973−8981.
49. Smith, C. A., and Rayment, I. (1996) *Biochemistry 35*, 5404−5417.
50. Holmes, K. C. (1997) *Curr. Biol. 7*, 112−118.
51. Löster, K., Baum, O., Hofmann, W., and Reutter, W. (1995) *FEBS Lett. 373*, 234−238.
52. Löster, K., Hofmann, W., Calvete, J. J., and Reutter, W. (1996) *Biochem. Biophys. Res. Commun. 229*, 454−459.
53. Bertrand, R., Derancourt, J., and Kassab, R. (1994) *FEBS Lett. 345*, 113−119.
54. Crevel, M.-T. C., Lockhart, A., and Cross, R. A. (1996) *J. Mol. Biol. 257*, 66−76.

BI970615H